Wave propagation in an hydrocarbon reservoir during exploitation: A a preliminary, integrated study

INTRODUCTION

Problem of reservoir estimation. The optimal exploitation of hydrocarbon reservoirs requires the accurate estimation of the reservoir's characteristics. Placement of wells, injection of gas and water, and production rate of hydrocarbons depend on the correct assessment of the reservoir properties. Furthermore, the field's properties change over time as reservoir pore fluid is removed.

I advocate to assess a reservoir's state by an integrated inversion of combine well test, well log, and seismic data. This paper is result of my exploratory reading and discusses the physics of reservoir flow and seismic wave propagation in porous rocks. The paper includes simple finite difference simulations for reservoir fluid flow and wave propagation.

Overview over various sections.

Inversion. The section on inversion considers when inversion problems should be integrated and when they should be separated.

Reservoir flow simulator. The section on reservoir flow simulation canvasses the fundamental equations based on Darcy's law, mass conservation, and gas-oil-water mixtures (black oil model). Additionally, the section introduces a simple simulator for a single phase fluid that I implemented.

Wave equation for porous rocks. The third section considers wave propagation in a porous rock medium. Central to the section is Gassmann's velocity expressions. Additionally, the section discusses Biot's derivation of frequency dependent wave equation for a saturated porous rock. The section discusses a simple implementation of an acoustic wave simulator.

A first experiment. The final section simulates the fluid flow and seismic time-lapse experiments over a simple reservoir model. For lack of time, the example currently simplifies much of the theory discussed in the paper. The historic success of simple models in seismic analysis encourages such a simplified first attempt.

Darcy-Gassmann-Elastic formulation Several competing physical models of porous rocks exist. The models usually vary in their assumptions and their mathematical sophistication. A scientist ought to choose the most parsimonious model for the experiment. The popular Darcy-Gassmann-Elastic formulation combines the feasible state of the art of all three fields into a single model. The formulation of the reservoir flow and Gassmann's elastic parameters are directly based on macroscopic models of porous rock. However, it is unclear if the combination of the three formulations is computationally feasible or parsimonious.

The formulation and implementation of the seismic and well simulation is my first step towards a future inversion of experimental field data. All simulators are implemented in Jest (Schwab and Schroeder, 1997), an inversion framework. The simulators are semi-linear operators and contain the adjoint operator of their linear projections.

Literature. Landa (Landa, 1997) discusses a sequence of synthetic two-dimensional test cases that integrate a petroleum engineer's well observations and estimates of pore saturation. While working out the inversion of well data in great detail, Landa assumes that geophysicists hand him the saturation data presumably derived from seismic time-lapse experiments. In contrast, I advocate the integration of the seismic and well experiments into a single inversion of a consistent reservoir model.

Lumley (Lumley, 1995) independently migrates several time-lapse surveys and shows the effect of changing pore fluids on migrated sections. He finally speculates about the interpretation of the observed amplitude changes in the seismic difference image. The difference section show clear reservoir changes. However, Lumley's field data is unusually well suited: the reservoir is extremely shallow, the target area is small. He does not combine the migrations into a single inversion, nor does he integrate any data from other physical experiments.

Biondo et al (Biondi et al., 1996) simulate and invert synthetic data based on a 3-D reservoir model. However, the inversion is not integrated in a single consistent formulation.

Motivation. I personally wrote this paper to learn about reservoir flow and wave propagation in porous rocks. Additionally, I include in the paper a short discussion of simulation and inversion of physical experiments. I believe that inversion theory is the key to integrate the various observations by geoscientists and petroleum engineers into a single earth model.

Wave propagation aspect. How does the integration of seismic and well experiments relate to a course in linear wave propagation? The formulation of the seismic experiment is based on the fundamentals taught in the course. The wave simulator implements the standard acoustic wave equation. The paper extends the course's discussion of homogenous and random media, to fluid filled porous media. Finally, the article's future inversion aspects complement the course's corresponding simulation techniques. I wanted to do this work, ever since reading Landa's thesis and, I admit, the course on wave propagation gave me the necessary excuse and motivation.

RESERVOIR FLUID FLOW SIMULATOR

[1] Unfortunately, a reservoir is difficult to access. It is buried hundreds or thousands of meters in the subsurface. A geoscientist only chance to access the reservoir directly is in a well. Petroleum engineers carefully observe a well's production volumes of oil, water, and gas. Additionally, the engineers measure pressure in the well or even conduct pressure tests. My discussion of reservoir fluid flow processes follows Landa (1997) and Aziz (1979).

Black-oil model. Petroleum engineers use various reservoir fluid flow simulators to relate their observations to reservoir properties, such as permeability, porosity, pressure distribution, and saturation. The *standard* black-oil model for a reservoirs mix of fluids comprises three distinct phases: oil, water, and gas. The oil phase dissolves a certain amount of gas; the water does not. Intuitively, one might want to describe the reservoir properties at the scales of pores. However, the traditional approach homogenizes the pore-scale heterogenities to macroscopic descriptions such as Darcy's law.

The general **equation of mass conservation**

$$-\nabla(\rho\mathbf{u}) = \partial_t(\rho\phi) + \tilde{q} \tag{1}$$

asserts that any local change in the flow of mass is due to a local source (or sink) $\tilde{q}$ or a temporal change in density or porosity. The source $\tilde{q}$ is a location's local well production which is zero for any location without a producing well. The vector $\mathbf{u}$ is the fluid flux, and ρ is the fluid density.

Darcy's law expresses the fluid flux in terms of pressure and gravity

$$\mathbf{u} = -\frac{k}{\eta}(\nabla p - \rho g \nabla z) \tag{2}$$

where k is the permeability, and η is the viscosity. The second term on the right hand side incorporates the gravitational effect, where g is the gravitational acceleration. Darcy's law is only valid for slow flow rates, where turbulence and inertia are negligible. Darcy's law 2 generalizes to the flow of multiple phases – oil, water, gas – in a porous rock:

$$\mathbf{u}_j = -\frac{kk_{rl}}{\eta_j}(\nabla p_j - \gamma_j \nabla z)\text{for } j = o, w.g$$

where k_{rl} is the relative permeability of each phase. The relative permeability is a function of saturation. Aziz (1979) discusses various empirical expressions for that dependency.

The combination of Darcy's law with the mass conservation equation 1 yields the fluid flow equations:

$$\nabla[\gamma_o(\nabla p_o - \rho_o g \nabla z)] \;\; = \;\; \partial_t[\frac{\phi S_o}{B_o}] + q_o$$

[1] The discussion in this section is not a thorough derivation of the equations, but the summary of my exploratory reading.

$$\begin{aligned}
\nabla[\gamma_w(\nabla p_w - \rho_w g \nabla z)] &= \partial_t[\frac{\phi S_w}{B_w}] + q_w \qquad (3)\\
\nabla[R_s\gamma_o(\nabla p_o - \rho_o g \nabla z) + \gamma_g(\nabla p_g - \rho_g g \nabla z)] &= \partial_t[\phi \frac{R_s S_o}{B_o}\frac{S_g}{B_g}] + R_s q_o + q_{fg}.
\end{aligned}$$

The equations relate differences in pressure gradient – left hand side – to temporal changes in pore saturation – right hand side. The equations are complemented by three additional constraints

$$\begin{aligned}
1 &= S_o + S_w + S_g\\
p_o - p_w &= f(S_w, S_g) \qquad (4)\\
p_g - p_o &= f(S_w, S_g)
\end{aligned}$$

The first equation states that the rock is saturated by the three fluids. The two bottom equations relate capillary pressures and saturations and are usually empiric (Aziz and Settari, 1979).

The parameters B_j relate parameter values at surface conditions – indicated by index S – and reservoir condition – indicated by index R. The parameters are defined as volume ratio

$$\begin{aligned}
B_o &= \frac{[V_o]_R + [V_{dg}]_R}{[V_o]_S} = f(p_o)\\
B_w &= \frac{[V_w]_R}{[V_w]_S} = f(p_w) \qquad (5)\\
B_g &= \frac{[V_g]_R}{[V_g]_S} = f(p_g)
\end{aligned}$$

and are based on the pressure-volume-temperature (PVT) constant at thermodynamic equilibrium. The first equation deviates from the other two since it accounts for the dissolved gas volume V_{dg}. The volume ratios B_j let us relate the density at reservoir conditions to the density at surface conditions:

$$\begin{aligned}
\rho_o &= \frac{\rho_{oS} + R_s \rho_{gS}}{B_o}\\
&= \hat{\rho}_o + \hat{\rho}_{dg} \qquad (6)\\
\rho_w &= \frac{\rho_{wS}}{B_w}\\
\rho_g &= \frac{\rho_{gS}}{B_g}
\end{aligned}$$

The mass transfer between the oil and gas phase is defined as $R_s = [V_{dg}/V_o]_S$.

The B_j ratios, and the mass transfer R_s, depend on the pressure p_j of the various phases $j = o, w, g$. Since water compressibility is small, the relationship $B_w = f(p_w)$ can be approximated by

$$B_w = \frac{B_{wb}}{1 + c_w(p_w - p_{wb})}.$$

The analogue expressions for B_o, B_g, R_s, and η_j are empiric and again discussed by Aziz and Settari (1979).

The coefficients γ_j in equation 4 express transmissibilities and are defined as

$$\gamma_j = \frac{k_{rl}}{\eta_j B_j} k.$$

Viscosities η_j of oil and gas strongly depend on temperature and pressure. The pressure dependency is again empirical Aziz and Settari (1979). The viscosity's temperature dependence is especially important in thermal-recovery processes such as steam injections. In general, the temperature dependency is well approximated by

$$\eta = \eta_0 (\frac{T}{T_0})^c$$

where η_0 and T_0 are reference points and c is a fluid specific constant.

Finally, porosity is often pressure dependent

$$\phi = \phi_0 \exp(c_R(p - p_0)) \approx \phi_0[1 + c_R(p - p_0)]$$

where c_R is the bulk compressibility of the rock and the porosity ϕ_0 and ρ_0 refer to known reference values.

The equations

$$\begin{aligned} \tilde{q_o} &= q_o \rho_{oS} \\ \tilde{q_w} &= q_w \rho_{wS} \\ \tilde{q_g} &= q_g \rho_{gS} + q_o R_s \rho_{gS} \end{aligned} \tag{7}$$

relate the in situ volumes $\tilde{q}$ of equation 1 to the production volumes q as they appear at the well head under standard surface condition.

Well observations. In a field experiment, petroleum engineers control the pressure in the well. Petroleum engineers conduct well tests by changing the pressure in the well and observing the reaction of the surrounding reservoir pressure (respectively its effect on the controlled well pressure). These experiments attempt to estimate local reservoir transmissibility but do have to account for the *skin effect*: the alterations of the rock next to the well. Additionally, petroleum engineers record the well's production volumes. The production volumes depend on the reservoir pressure p and the well bore pressure $p_w f$:

$$q B \Delta t - \frac{k \Delta t}{\eta} \int \int \frac{\partial p}{\partial n} dS = C \Delta p_w f$$

where q the volume production rate per unit of time at the surface (not at reservoir pressure), B is the formation volume factor, C represents the ability of the well bore to store fluids, n is the normal of the well bore, S the well bore's surface.

I hope to combine such well observations with seismic time-lapse data to yield improved estimates of reservoir property maps.

Simplified well system My preliminary implementation is based on the assumption that the reservoir only contains a single fluid, e.g. oil but neither water, nor gas. This assumption might be locally reasonable for large oil fields, albeit I expect almost all hydrocarbon mixtures to release gas when a production lowers the reservoir pressure sufficiently. The assumption of a single fluid phase collapses the fluid flow equations 4 and its constraints 4 to a single equation.

Additionally, I neglect gravitational forces ($g = 0$). I assume that the rocks transmissibility γ varies smoothly and that the rocks pore volume is independent of pressure ($c_R = 0$). Finally, I suggest that the reservoir fluid is only slightly compressible and consequently satisfies

$$\frac{\rho}{\rho_0} = \frac{B_0}{B} = \exp(c_f(p - p_0)) \approx 1 + c_f(p - p_0).$$

Under these assumption the equation system for multiple phases collapses to the diffusivity equation

$$\nabla^2 p = \frac{\phi \eta c_f}{k} \partial_t p + \frac{\eta}{\rho k} + \tilde{q}. \tag{8}$$

This single phase fluid flow equation for porous rocks can be derived directly from the corresponding versions of Darcy's law and the mass conservation (Raghavan, 1993).

I doubt that seismic field data can detect reasonable changes in pressure and density of a single fluid phase around a well. Instead, current time lapse surveys concentrate on detecting saturation changes in multi-phase reservoirs, that often involve gas, steam, or highly pressured water. I chose the single fluid phase case since it is the simplest to implement. Should I continue this work, I will seek the collaboration of an experienced petroleum engineer to improve the reservoir flow simulator. The simplicity of the reservoir model, however, might prove beneficial when formulating the inverse problem.

Parameterization My simple reservoir simulator requires as input a transmissibility map of the reservoir, an initial pressure distribution within the reservoir (usually assumed to be constant), the pressure history at the boundary of the wells. Given these parameters, the simulator computes the reservoir pressure distribution over time. For this preliminary study, I restrict the reservoir to a two-dimensional plane. The model is computationally manageable, and the results can be visualized effectively.

Implementation of a reservoir flow simulator

The finite difference reservoir flow simulator for a single phase is a straightforward explicit finite difference implementation of the corresponding fluid flow equation 8:

$$u_{t+1}^{x,y} - u_t^{x,y} = \hat{d}[(u_t^{x-1,y} - 2u_t^{x,y} + u_t^{x+1,y}) + (u_t^{x,y-1} - 2u_t^{x,y} + u_t^{x,y+1})]$$

where $\hat{d} = d\Delta t/\Delta^2$ is the transmissibility. Each grid point represents a homogeneous subsurface cell. A straightforward stability analysis (see the finite difference wave equation section) yields $\hat{d} \leq 1/4$ and $\hat{d} > 0$. Figure 1 shows snapshots of a reservoir of constant transmissibility and random sources of pressure. The pressure impulses diffuse over time as we would expect from a solution to a parabolic differential equation.

A first reservoir flow simulation experiment

Figure 2 shows the transmissibility of a first simple reservoir model. The transmissibility is increased in an elliptic area in the center. Such high transmissibility region may be caused by sand deposits within a paleochannel.

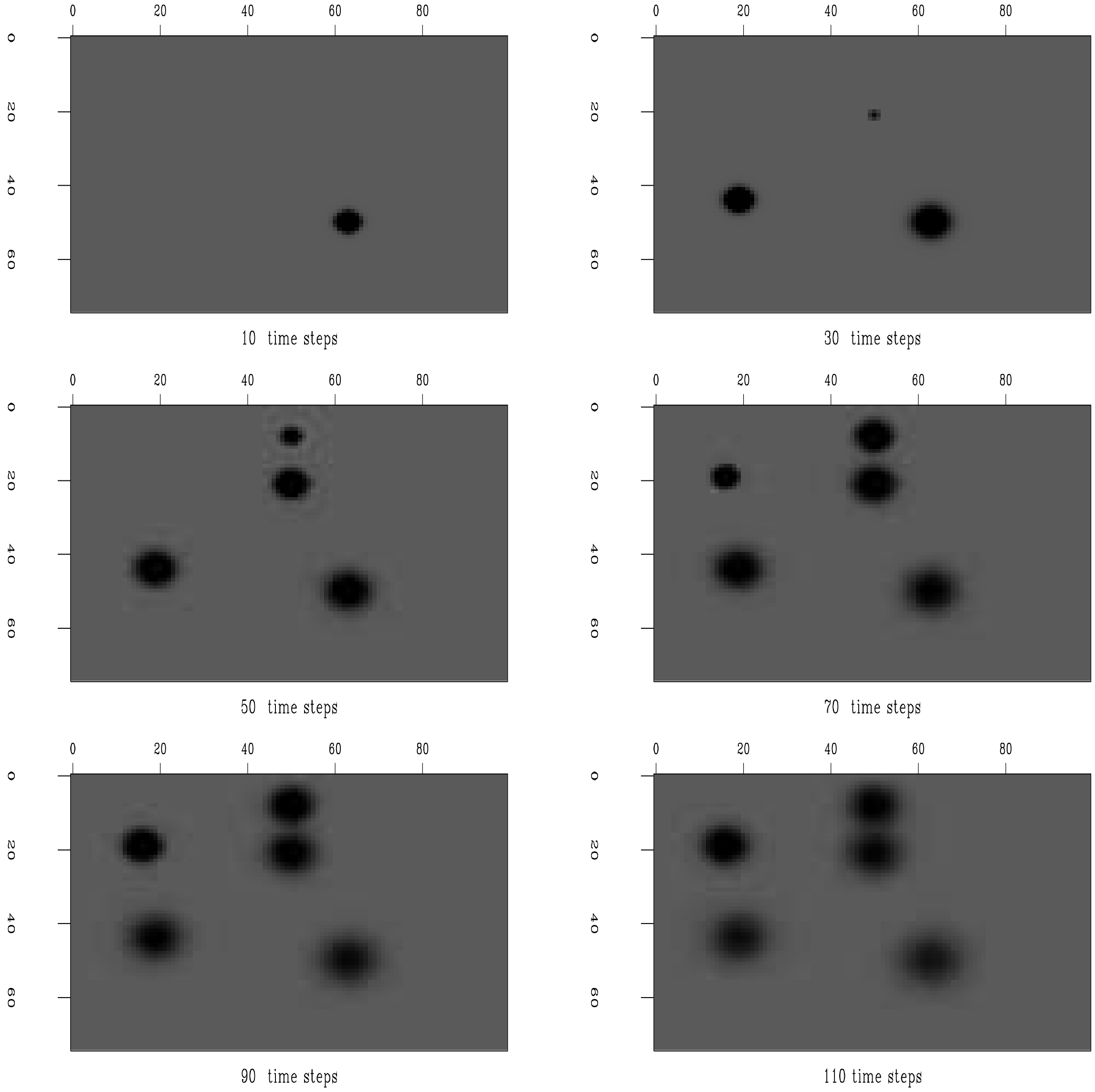

Figure 1: Snapshots of the reservoir fluid flow simulator for a medium of constant transmissibility and randomly located point sources of pressure. The panels show the pressure field as time increases from left to right and top to bottom. An impulsive source generates an impulse that diffuses over time. $\boxed{\text{impFlowSnap}}$ [ER]

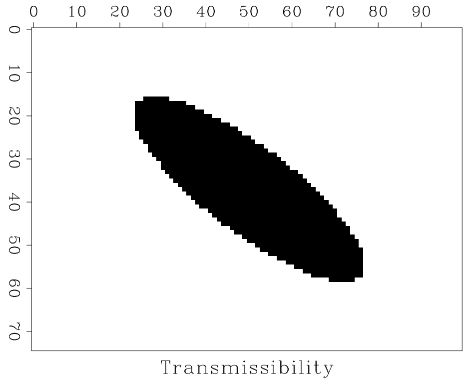

Figure 2: Transmissibility map of the two-dimensional reservoir. The fluid will flow more rapidly in the elliptic shape in the center of the reservoir. $\boxed{\text{transmissibility}}$ [ER]

I chose to drill two wells into the reservoir: each well is located within the high transmissibility area. One of the wells adds fluids (source), the other one extracts fluids (sink). The snapshots in Figure 3 show the areas of increased pressure or fluid density.

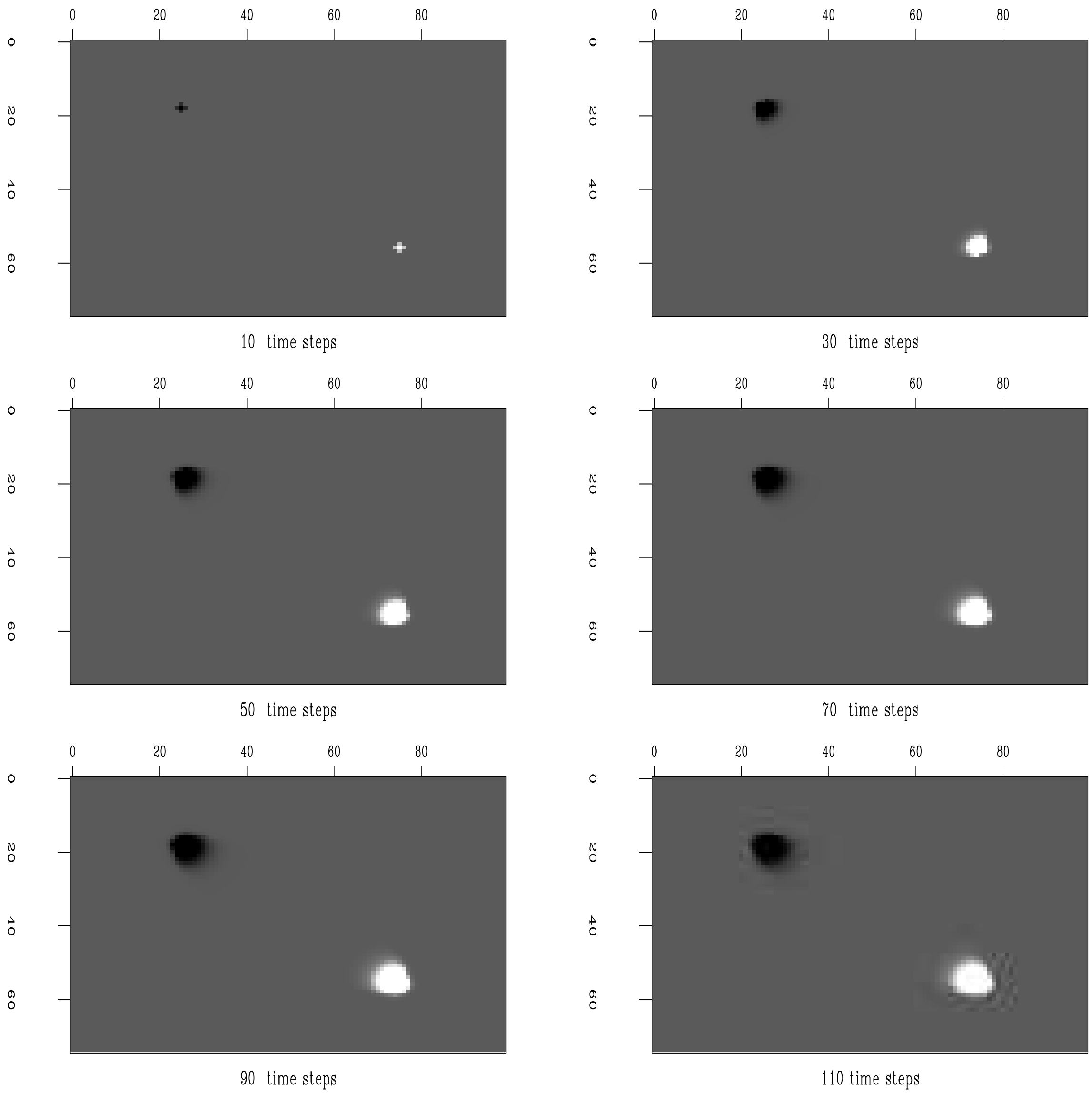

Figure 3: Snapshots of the reservoir fluid flow simulator. The simulation includes two wells: The northern well adds fluid to the subsurface increasing the pressure around the well, the southern well extracts fluid and lowers the local pressure. I arbitrarily positioned the two wells at the foci of the reservoir's elliptic high transmissibility region. resFlowSnap [ER]

SEISMIC WAVE SIMULATOR

Seismic experiments complement well measurements. Seismic surveys record the continuous wavefield generated by impulsive sources and reflected or transmitted by geological subsurface layers. Traditionally, the recorded data is processed to reveal the structure of the three-dimensional subsurface geology. In the past decade, geophysicists developed additional seismic processing methods to estimate concrete subsurface rock properties, such as the ratio of compressional and shear wave velocity or bulk modulo or even density (**?**). Recently, geophysicists employ repeated seismic surveys over an actively exploited field to estimate changes in the reservoir's fluid contents. Assuming that the reservoir rock is unchanged, such time-lapse or 4-D experiments relate subtle wavefield differences to reservoir fluid changes. Unfortunately, seismic surveys themselves are complex field experiments that are difficult to repeat exactly. Variations in recording geometry, instrumentation, and wave source may lead to wavefield variations that are falsely interpreted as changes in reservoir fluid contents.

Wave equation. For this study, I chose Gassmann's formulation of the wave equation for porous rock. Gassmann's formulation resembles the formulation for homogeneous rocks and is widely used in rock physics studies. Furthermore, Gassmann's formulation shares a parameterization similiar to the parameterization for reservoir fluid flow simulations.

The generic wave equation for an isotropic, linear, elastic medium is

$$(K + \frac{4}{3}\mu)\nabla^2\mathbf{u} - \mu\nabla \times \nabla\mathbf{u} = \rho\ddot{\mathbf{u}} \tag{9}$$

where K is the materials bulk modulo and μ is its shear modulo. This equation approximates the wave propagation in many non-isotropic, non-linear, and non-elastic materials if the heterogenities of the material and the ampltiude of the wave are small compared to the wave's wavelength.

The solutions to the isotropic wave equation can be separated into a compressional mode ($\mathbf{u} = \nabla\Theta$) and a shear mode ($\mathbf{u} = \nabla \times \Theta$). Substitution of these two modes into the isotropic wave equation 9 yields the same simplified wave equation

$$\nabla^2\Theta = \frac{1}{v^2}\ddot{\Theta}. \tag{10}$$

but with two distinct distinct propagation velocities $v = v_s$ and $v = v_p$. In terms of the material parameters of the isotropic wave equation the compressional wave velocity is

$$v_p = \sqrt{\frac{K + \frac{4}{3}\mu}{\rho}} \tag{11}$$

and the shear wave velocity is

$$v_s = \sqrt{\frac{\mu}{\rho}}. \tag{12}$$

Gassmann show's that these equations for homogeneous isotropic material approximate the wave propagation in porous rocks if the material parameters are the appropriate averages of the rock's constituents.

The density of the porous rock

$$\rho = \phi \rho_{fl} + (1 - \phi) \rho_{min} \tag{13}$$

is the average of the fluid density ρ_{fl} and the rock matrix density ρ_{min} weighted by the porosity ϕ. In the case of oil, water, and gas – the petroleum engineer's black oil model – the fluid density is the average of the density of the various components weighted by their saturation:

$$\rho_{fl} = S_g \rho_g + S_o \rho_o + S_w \rho_w. \tag{14}$$

According to Gassmann, the effective bulk modulo of the saturated porous rock K_s is a weighted average of the bulk modulo of the dry rock skeleton K_d , the bulk modulo of the constituent mineral material K_m , and the bulk modulo of the saturating fluid K_f

$$\frac{K_s}{K_m - K_s} = \frac{K_d}{K_m - K_d} + \frac{K_f}{\phi(K_m - K_f)}. \tag{15}$$

Isolating the unknown K_s yields

$$K_s = K_d + \frac{(1 - b)^2}{(1 - \phi - b)/K_m + \phi/K_f}$$

where $b = K_d/K_m$. The bulk modulo of an oil-water-gas fluid mixture is the average

$$\frac{1}{K_f} = \frac{S_g}{K_g} + \frac{S_o}{K_o} + \frac{S_w}{K_w}, \tag{16}$$

where $S_{g,o,w}$, $K_{g,o,w}$, $\rho_{g,o,w}$ are the saturations, bulk moduli, and densities of gas, oil, and water phases.

Finally, the shear moduli of the saturated rock is unchanged by the fluid pore contents

$$\mu_s = \mu_d. \tag{17}$$

The expressions satisfy the limiting cases. A solid medium implies $\phi = 0$ and $K_f = K_s = K_m$. A fluid medium implies $\phi = 1$ and $K_m = 0$ and $K_s = K_f$. Gassmann's expressions approximate a porous rock only at low frequencies and is strictly valid only in the static (zero-frequency) case. The given averages only approximate the properties of a saturated rock, if the phases in the computational cell are mixed uniformly at very small scale.

Problems and hope for formulation The formulation of a porous rock model does not guarantee its applicability in practice. Traditional AVO studies have shown that seismic reflection experiments are rather insensitive to density changes. Furthermore, the drastic amplitude effect of gas saturation is insensitive to the amount of gas: large and small gas saturations cause almost the same bright spots in seismic sections (?). In general, traditional seismic surface experiments resolved little beyond reflectivity and compressional wave velocity. However, the innovation of time-lapse experiments gives seismic experiments a particular sensitivity to saturation changes. However, the optimal formulation of the simulation and inversion problem is still unclear.

IMPLEMENTATION OF A WAVE SIMULATOR

I implemented a finite-difference simulator for the rudimentary acoustic two-way wave equation 10. For my preliminary exploits, I chose a 2-D plane. The finite difference simulator computes the wavefield for arbitrarily placed sources. I intend to first model simple transmission experiments, possibly with plane waves. Seismogramms for various acquisition geometries are easily extracted from the complete wavefield.

Following Gassmann's model, the fluid saturated, porous rock properties enter the simulator by defining the velocity field v of equation 11. In particular, Gassmann's bulk modulo and density depend on the fluid saturation S_o, S_w and S_g. I assume that the fluid flow in a producing reservoir and the wave propagation of a seismic experiment are decoupled, since both processes happen on very different time scales and are limited to small, linear motions. Consequently, I assume the saturation and the dependent velocity as fixed during a seismic experiment. However, I expect that the saturation and consequently the velocity of the reservoir rocks possibly changes between subsequent experiments.

I implemented the finite difference simulator as part of Jest (Schwab and Schroeder, 1997), a Java inversion library. The linear simulators contain their adjoint operator that are checked by the dot product test.

Finite difference wave equation. I implement the acoustic scalar wave equation

$$\ddot{\sigma} = v^2 \nabla^2 \sigma \tag{18}$$

as a finite difference formula which is second-order accurate in space and time

$$\sigma_{t+1}^{x,y} - 2\sigma_t^{x,y} + \sigma_{t-1}^{x,y} = \hat{v}^2[(\sigma_t^{x-1,y} - 2\sigma_t^{x,y} + \sigma_t^{x+1,y}) + (\sigma_t^{x,y-1} - 2\sigma_t^{x,y} + \sigma_t^{x,y+1})]$$

where $\hat{v} = v\Delta t/\Delta x$. Isolation of $\sigma_{t-1}^{x,y}$ and addition of identical terms yields the final difference formula

$$\sigma_{t+1}^{x,y} = (2 - 4\hat{v}^2)\sigma_t^{x,y} + \hat{v}^2[(\sigma_t^{x-1,y} + \sigma_t^{x+1,y}) + (\sigma_t^{x,y-1} + \sigma_t^{x,y+1})] - \sigma_{t-1}^{x,y}. \tag{19}$$

The Figure 4 shows snapshots of a constant velocity wavefield that is excited by random point sources.

Boundary conditions. I also implemented Clayton and Engquist's (1980) absorbing boundary conditions. The absorption of the wave is due to a subtle change of the material coefficients at all edge points of the computational grid. While the interior coefficients implement the two-way wave equation, the boundary points implement the paraxial one-way wave equation. The one-way wave equation propagates the energy outwards but not

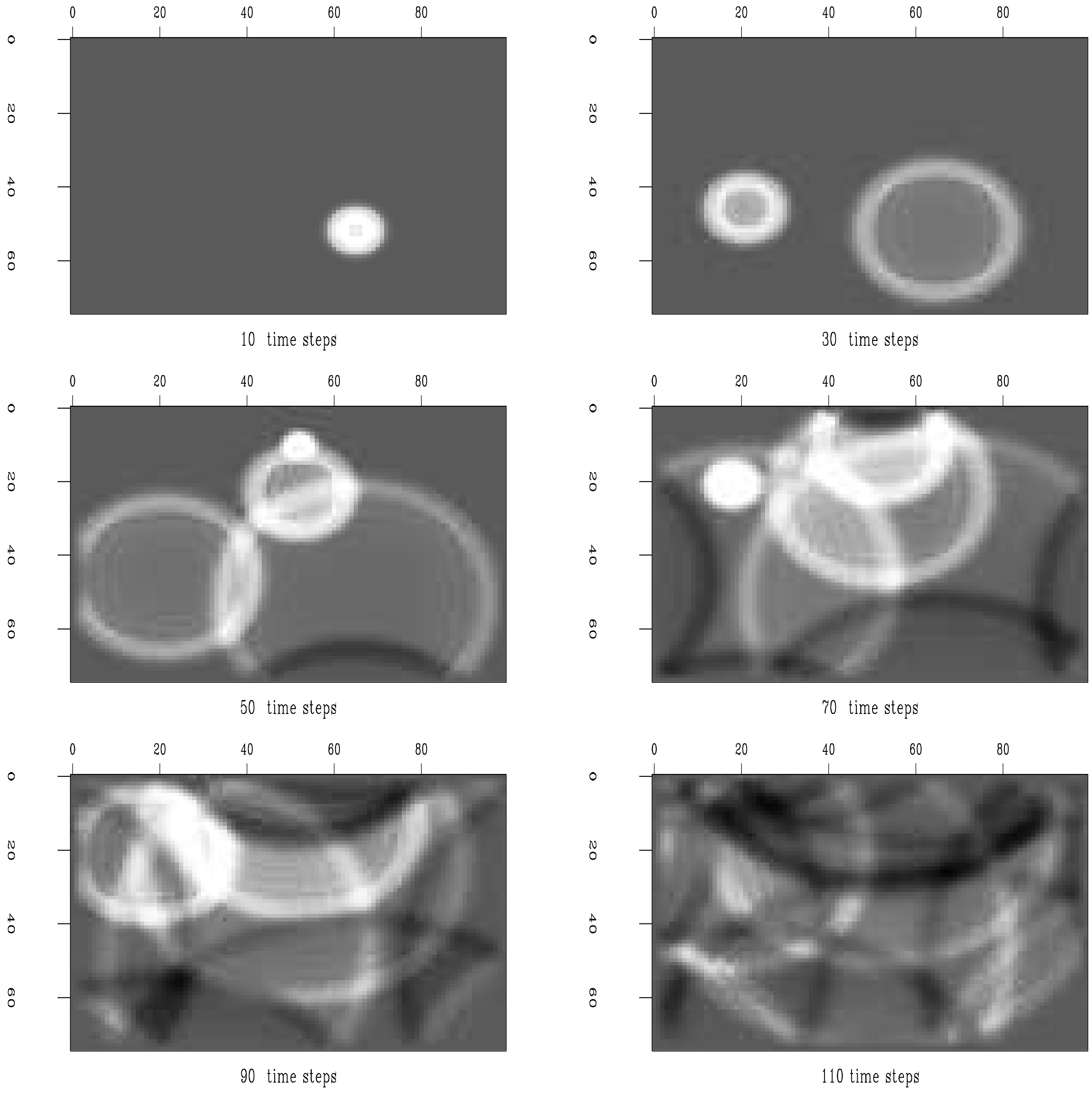

Figure 4: Snapshots of the acoustic wave equation simulator for a constant propagation medium and randomly located point sources. The panels show a wavefield as time increases from left to right and top to bottom. An impulsive source generates an impulse that propagates spherical wavefronts (Scaling of the image might make the wavefront appear elliptical). The wavefront is reflected at the boundary. impWaveSnap [ER]

inwards. Unfortunately, I am currently baffled since my implementation does not absorb the energy as promised.

Stability analysis. The fundamental solution to the difference equation above is

$$\sigma_t^{x,y} = \xi^t e^{ik_x j\Delta x} e^{ik_y l\Delta y} \sigma_0. \tag{20}$$

The value of ξ has to be less or equal 1 to ensure that the solution does not grow exponentially with t (Courant-Friedrichs-Levy condition). Substitution of the fundamental solution into the difference equation 19 yields

$$0 = \xi^2 + [(2 - 4\hat{v}^2) + \hat{v}^2(e^{-ik_y\Delta y} + e^{ik_y\Delta y} + e^{ik_x\Delta x} + e^{-ik_x\Delta x})]\xi + 1. \tag{21}$$

This equation is a quadratic polynomial in ξ. The quadratic has a real solution only if its determinant is greater or equal than 0. Since

$$e^{-i\phi} + e^{i\phi} = 2\cos\phi$$

we can write the determinant as

$$0 \le [2(1 + 2\hat{v}^2(u - 1)]^2 - 4$$

where $u = (1/2)(\cos k_x\Delta x + \cos k_y\Delta y) \in [-1, 1]$. Isolation of $\hat{v}^2$ leads to

$$\frac{1}{2} \ge \hat{v}^2$$

where we divided once by $(u - 1) \le 0$. In summary, the finite difference computation is stable as long as $\hat{v} = v\Delta t/\Delta x$ is smaller than $1/\sqrt{2}$. This expression might be used to choose Δt for a given velocity v and a desired output interval Δx.

Implementation. The finite difference equation 19 expresses a recursive computation in time of the wavefield σ over time:

$$\sigma_t = a\sigma_{t-1} + b\sigma_{t-2} + \mathbf{s}_t \tag{22}$$

where $\mathbf{s}_t$ is the known source contribution at time t. The vectors σ_t and $\mathbf{s}_t$ refer to constant time instances of the spatial (x, y) grid. The equation expresses only the time dependency of the recursion explicitly: the straightforward spatial convolution of the original finite difference equation is symbolically represented by the coefficients a and b.

Figure 5 indicates how the algorithm recursively computes the values in the red plane from the earlier green and blue plane. The first two time planes implement the initial conditions. Once the entire cube is computed, a constant time plane contains a snapshots of the wavefield. The extraction of all wavefield values that correspond to a (x, y)-location yields a time dependent seismogram.

The recursion 22 is a handy approach to compute the wave solution σ of the fundamental operator equation

$$\mathbf{A}\mathbf{s} = \sigma. \tag{23}$$

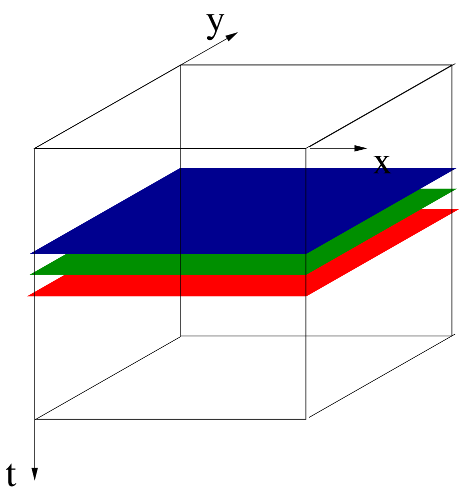

Figure 5: Computational grid. The domain and range of the finite difference implementation is an identical cube of (x, y, t) values. The input cube contains the source amplitudes of any point in time and space. The output cube contains the wavefield amplitude of any point in time and space. The values in the red plane are computed from the values of the green and blue plane according to the difference equation 19. $\boxed{\text{cube}}$ [NR]

Because of the operator's recursive definition, we do not know its explicit matrix form $\mathbf{A}$. However, the recursion 22 is easily reformulated to

$$\mathbf{s}_t = \sigma_t - a\sigma_{t-1} - b\sigma_{t-2}$$

which corresponds to the matrix expression $\mathbf{s} = \mathbf{A}^{-1}\sigma$ or

$$\begin{bmatrix} s_0 \\ s_1 \\ s_2 \\ s_3 \end{bmatrix} = \begin{bmatrix} 1 & \cdot & \cdot & \cdot \\ -a & 1 & \cdot & \cdot \\ -b & -a & 1 & \cdot \\ \cdot & -b & -a & 1 \end{bmatrix} \begin{bmatrix} \sigma_0 \\ \sigma_1 \\ \sigma_2 \\ \sigma_3 \end{bmatrix}. \tag{24}$$

In summary, we have a recursive formula to compute σ from $\mathbf{s}$ but we lack a simple explicit matrix expression. On the other hand, we know a simple explicit matrix expression that computes $\mathbf{s}$ for a given σ.

How do we find an expression for the adjoint of $\mathbf{A}$? Since $(\mathbf{A}^{-1})' = (\mathbf{A}')^{-1}$, we yield an explicit expression for the inverse of the adjoint of $\mathbf{A}$ from 24:

$$\begin{bmatrix} \sigma_0 \\ \sigma_1 \\ \sigma_2 \\ \sigma_3 \end{bmatrix} = \begin{bmatrix} 1 & -a & -b & \cdot \\ \cdot & 1 & -a & -b \\ \cdot & \cdot & 1 & -a \\ \cdot & \cdot & \cdot & 1 \end{bmatrix} \begin{bmatrix} s_0 \\ s_1 \\ s_2 \\ s_3 \end{bmatrix}.$$

We can compute the actual adjoint of $\mathbf{A}$ by reformulating the matrix equation as a recursion

$$\sigma_t = \mathbf{s}_t - a\mathbf{s}_{t+1} - b\mathbf{s}_{t+2}$$

which we can rewrite as

$$\mathbf{s}_t = \sigma_t + a\mathbf{s}_{t+1} + b\mathbf{s}_{t+2}.$$

The adjoint recursion loops from later times to earlier times.

A first seismic simulation experiment

I implemented a simple acoustic wave simulator. An elastic wave simulator (which I chose not to implement) would be able to compute Gassmann's compressional and shear waves. Furthermore, such an elastic wave simulator would have nicely corresponded with the more sophisticated rock physics and reservoir flow considerations discussed in this paper. Alas, I did not have the time to implement the more complex operator. The simpler acoustic simulator may thrive nicely with my simple reservoir flow simulator. Furthermore, acoustic wave propagation has been surprisingly successful in traditional seismic processing.

The input to the wave simulator is a single velocity field. In this first draft, I derive the velocity field independent of the underlying rock physics considerations discussed here. I simply choose a constant base velocity and add a scaled version of the pressure field computed by the reservoir simulator. This approach assumes the velocity variation to be linearly dependent on reservoir pressure.

The wavefield source is a plane wave (Ricker wavelet) that initially originates at the northern edge of the reservoir. To simulate a more realistic seismic field experiment, I would use a series of point sources and extract from the complete wavefield time traces at specific geophone locations.

The first sesimic wavefield recorded over the initial reservoir, Figure 6, and the later wavefield recorded over an altered reservoir, Figure 7, show no apparent difference. The wavefield is dominated by the large amplitude of the direct wave. However, the difference of the two wavefields, Figure 8, reveals the secondary wavefield due to the scattering effect of the altered fluid contents of the rock adjacent to the two wells.

ALTERNATIVE ROCK VELOCITY MODELS

My decision to follow Gassmann's model is heuristic. I expect successful simulation and inversion of time-lapse data to justify the formulation. Ultimately, the careful study of the sensitivity and resolvability of reservoir parameters will have to decide the most feasible approach.

The wave equation governs the seismic experiment. It can be formulated for a wide variety of problems and materials. The literature offers simpler and more complex alternatives to Gassmann's formulation. Biot (1962), for example, offers a comprehensive theory that includes Gassmann as a special low-frequency case. Terzaghi offers an alternative approximation that is popular in geomechanic applications. Geerstma and Smit () approximate Biot's frequency dependent velocity expressions by a combination of a zero frequency and infinite frequency term. Mindlin (1949) approximates macro elastic modulo for porous rock from pore-scale considerations of dry dense random pack of identical spherical grains. Wyllies (1956), on the other hand, offers a simple velocity averaging scheme that is popular in well logging.

The list of available models of wave propagation in fluid filled porous rocks is long and

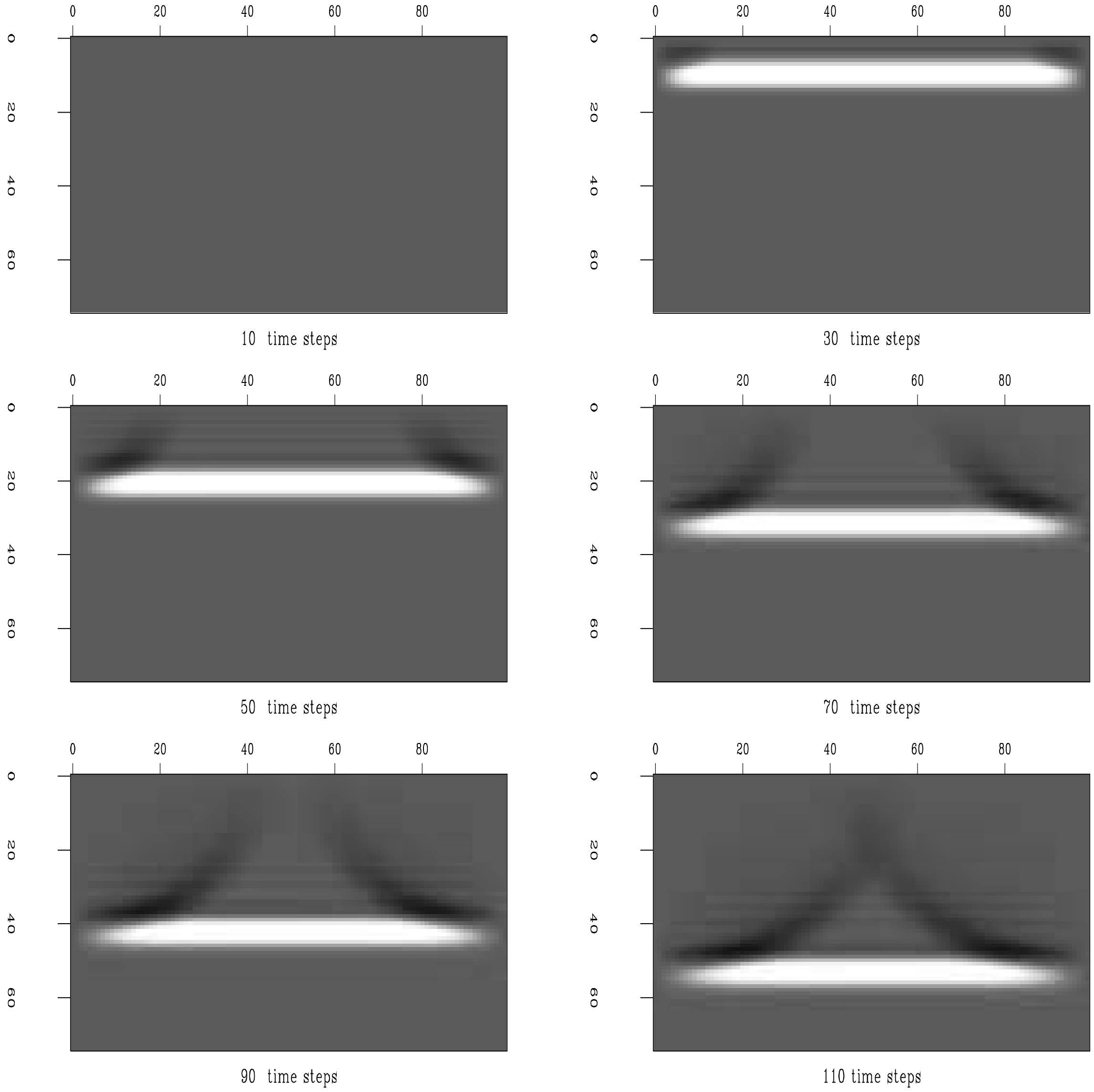

Figure 6: Snapshots of a plane wave before well production. A plane wave propagates unperturbed through the reservoir before the well production commences. The velocity field is constant. resWave1Snap [ER]

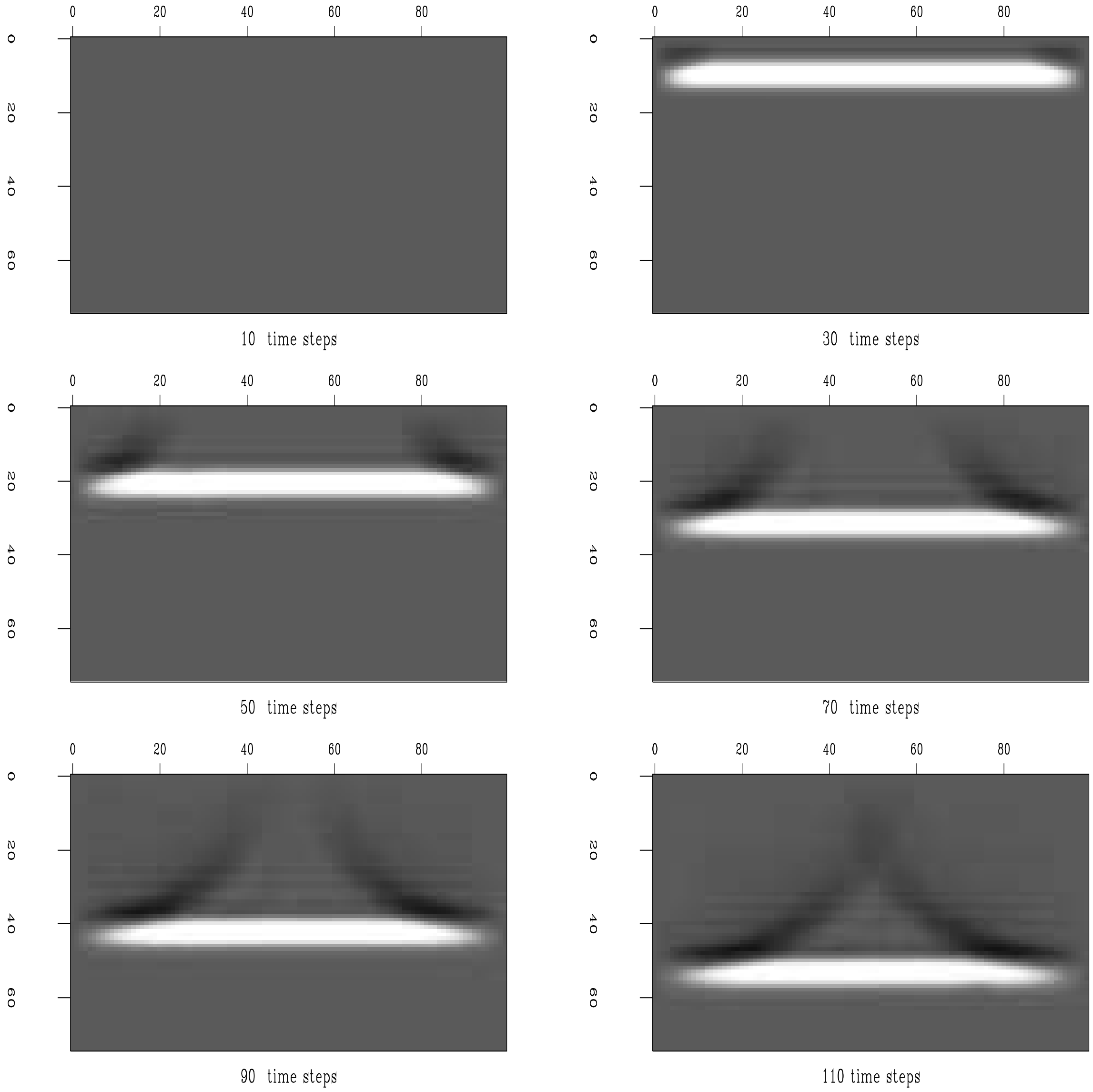

Figure 7: Snapshots of a plane wave after well production. A plane wave propagates through the reservoir after one well has increased its surrounding pressure and the other well has decreased it. The wave seems identical to the wave that propagates through the unperturbed reservoir. $\boxed{\text{resWave2Snap}}$ [ER]

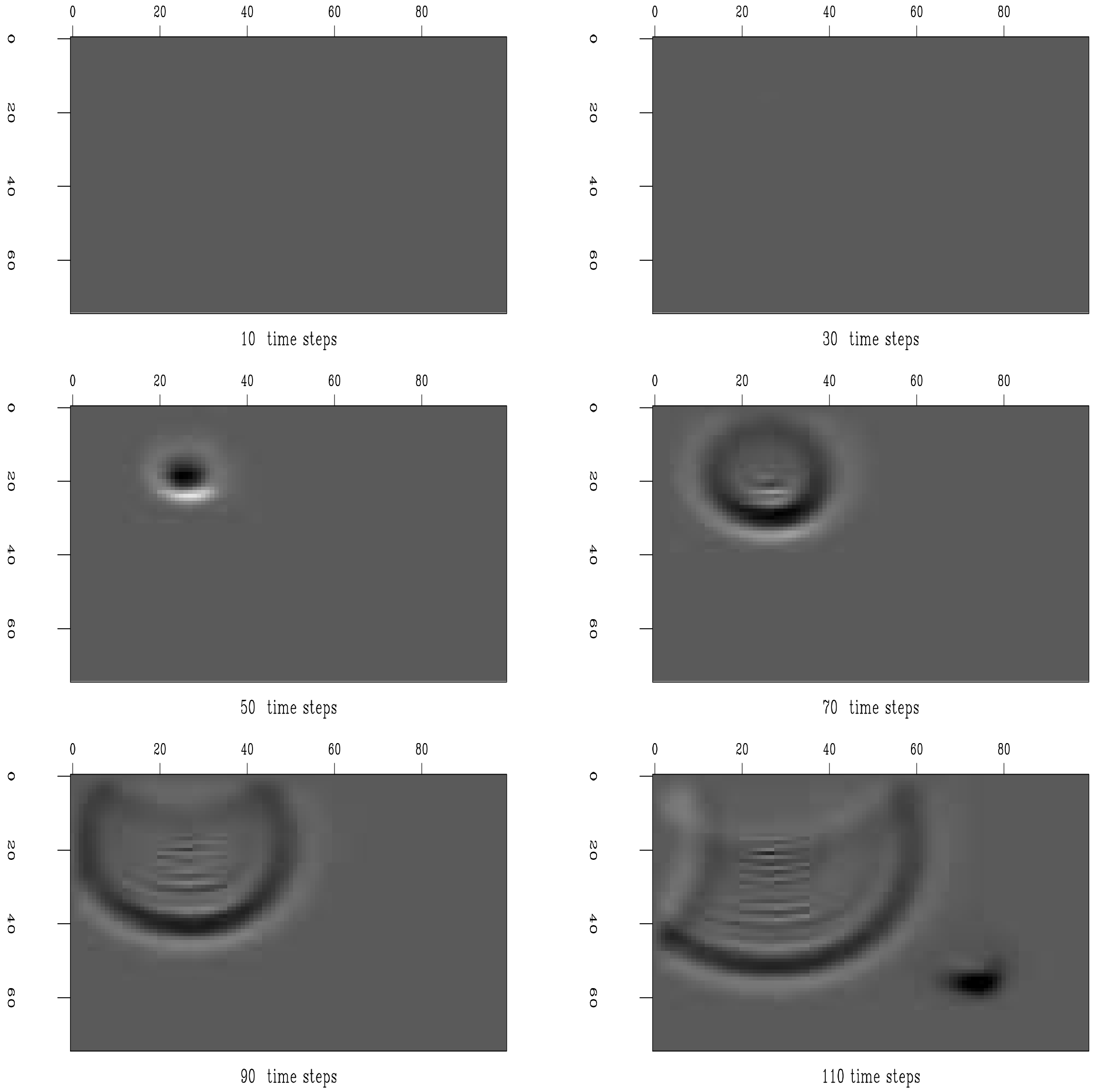

Figure 8: Difference between the snapshots. The difference of the two seismic wavefields reveals subtle effects due to the changed pressure field. The areas of changed pressure around both wells act as secondary waves and cause spherical waves to propagate outward from the well locations. resDiffSnap [ER]

I restrict my discussions to Gassmann (above), Biot, Terzaghi, and Wyllie. What follows are not mathematical derivations, but an overview and motivation of various formulations.

Biot's model

Biot's theory (Bourbie et al., 1987) is based on the fundamental assumption of continuum mechanics that the wavelength is large in comparison with the size of the macroscopic elementary volume of the material and that the displacement is small so that the strain tensor is linear. These continuum conditions are readily satisfied by seismic studies. Furthermore, Biot assumes that the rock matrix is elastic and isotropic, that the liquid phase is continuous, that the rock matrix is solid, that the pores are disconnected[2], and that the porosity is isotropic and uniform. These assumptions are approximately true for many subsurface rocks.

The **equation of continuity** for a porous rock is

$$\xi = -\nabla \mathbf{w}$$

where ξ is the local fluid increase due to the filtration of fluid $\mathbf{w}$. If $\mathbf{U}$ is the displacement of the liquid phase and $\mathbf{u}$ is the displacement of the solid phase, then the filtration velocity is

$$\dot{\mathbf{w}} = \phi(\dot{\mathbf{U}} - \dot{\mathbf{u}})$$

where ϕ is the rock porosity.

The **constitutive equation** is

$$\begin{aligned} \sigma_{ij} &= \lambda_0 \, trace(\epsilon)\delta_{ij} + 2\mu\epsilon_{ij} - \beta p \delta_{ij} && (25) \\ \xi &= \frac{1}{M} p + \beta \, trace(\epsilon) && (26) \end{aligned}$$

where $\lambda_0 = \lambda_f - \beta^2 M$. The coefficient μ is the standard shear modulus, which is independent of the fluid content. The coefficient λ_f is the second Lame coefficient for a *closed* rock sample – a rock sample filled with water and without any change in fluid contents ($\xi = 0$). Consequently, λ_f is linked to the elastic constants of the rock matrix and the fluid. λ_0 is the analogue coefficient for an open system – a system with no external pressure ($p = 0$). Coefficient M is the pressure required to increase the fluid content of a unit volume at iso-volumetric strain – $trace(\epsilon) = 0$. The coefficient β quantifies the proportion of pressure due to the variation in fluid content for an open system. It is linked to the porosity and the geometry of the flow channels. All these coefficients can be measured in the laboratory on rock samples. In the limiting case that $\beta = \xi = 0$ and $M = \infty$ we yield the constitutive relationship for a single solid phase.

The constitutive equation is derived from changes in the volumetric energy potential V due to infinitesimal increments in strain and fluid contents

$$dV = \frac{\partial V}{\partial \epsilon_{ij}} d\epsilon_{ij} + \frac{\partial V}{\partial \xi} d\xi = \sigma_{ij} d\epsilon_{ij} + p d\xi.$$

[2]This assumption contradicts the underlying model of a permeable reservoir. I need to ask a rock physicist.

where p is a pressure average in the fluid, $sigma$ is the macroscopic stress tensor. The isotropy of the rock permits an approximation of the general tensor relation by the tensors first two invariants (the tensor's trace is the first invariant). Introduction of the standard Lame coefficients yields the constitutive relation above.

The constitutive equation at zero fluid pressure $p = 0$ and at hydrostatic fluid pressure $p = -trace(\epsilon)$ yields relationships that when expressed in terms of the saturated bulk modulo K_s, the open or dry bulk modulo K_d, the bulk modulo of the fluid K_f, and the bulk modulo of the solid skeleton K_m can be combined to the Gassmann equation 15. The equations assume quasi-static behaviour and are only true for low-frequency waves.

The **equations of motion** for porous rocks are

$$\begin{aligned} \sigma_{ij,j} &= \rho\ddot{u}_i + \rho_f\ddot{w}_i && (27) \\ -p_{,i} &= \rho_f\ddot{u}_i + \rho_w\ddot{w}_i \\ +\frac{1}{\gamma}\dot{w}_i. & && (28) \end{aligned}$$

where σ is the stress, u is the displacement of the matrix, w is the displacement of the fluid, γ is the effective transmissibility (or hydraulic permeability or fluid mobility). The transmissibility is the ratio of the absolute rock permeability k and the fluid viscosity η: $\gamma = k/\eta$. The average density ρ is $\rho = (1 - \phi)\rho_s + \phi\rho_f$. The effective fluid density ρ_w takes the porosity and the shape of the pores into account. The coupling effect is usually described by

$$\rho_w = \frac{a}{\phi}\rho_f$$

where the tortuosity parameter $a \geq 0$ is the factor incorporating the pore shape. Tortuosity tends to 1 as the porosity tends to 1. Berryman (1980) suggested to apply the tortuosity expression for solid spherical particles

$$a = \frac{1}{2}[\frac{1}{\phi} + 1]$$

to porous rock.

If there is no average relative fluid movement with respect to the overall macroscopic movement of the rock, i.e. $\mathbf{w} = \mathbf{0}$, then the first equation of 28 is reduced to the standard single phase case. If the acceleration of the fluid and the rock are zero – $\ddot{\mathbf{u}} = \ddot{\mathbf{w}} = \mathbf{0}$ – the motion is a steady state flow and the second equation of 28 reduces to Darcy's classic law of fluid flow in permeable material.

Bourlie (1987) derives The equations of motion from a strain potential expression that yields the constitutive equation, a potential expression for dissipation, and a potential expression for kinetic energy.

Biot's **wave equation** is, as usual, derived by substitution from the equation of motion 28 and the constitutive equation 26:

$$\begin{aligned} (\lambda + 2\mu)\nabla^2\mathbf{u} + Y\nabla^2\mathbf{U} - \mu\nabla\times\nabla\times\mathbf{u} &= \rho_{11}\ddot{u} + \rho_{12}\ddot{\mathbf{U}} + b(\dot{\mathbf{u}} - \dot{\mathbf{U}}) && (29) \\ Y\nabla^2\mathbf{u} + R\nabla^2\mathbf{U} &= \rho_{12}\ddot{u} + \rho_{22}\ddot{\mathbf{U}} - b(\dot{\mathbf{u}} - \dot{\mathbf{U}}) \end{aligned}$$

where

$$\begin{aligned} \lambda &= \lambda_f + M\phi(\phi - 2\beta) \\ Y &= M\phi(\beta - \phi) \\ R &= M\phi^2 \\ \rho_{11} &= \rho + \phi\rho_f(a-2) \\ \rho_{12} &= \phi\rho_f(1-a) \\ \rho_{22} &= \phi\rho_f a \\ b &= \frac{\phi^2}{\gamma}. \end{aligned} \tag{30}$$

b is the coefficient governing the wave's energy dissipation which in Biot's system is entirely due to relative motion of the fluid and matrix components.

The equations reduce to the limiting case of a perfect fluid when $\phi = \beta = a = 1$, $\lambda_f = M$, and $\mu = b = 0$ (since γ tends to infinity and the viscosity tends to 0). Consequently, the first equation disappears of 30 and the second reduces to

$$M\nabla^2\mathbf{u} = \rho_f\ddot{\mathbf{U}}.$$

If the medium is solid, we have $\beta = \phi = 0$ and a tends to infinity. Consequently, the second equation of 30 yields

$$0 = -a\phi\rho_f\ddot{\mathbf{u}} + a\phi\rho_f\ddot{U} - b(\dot{\mathbf{u}} - \dot{\mathbf{U}})$$

while the first equation reduces to

$$(\lambda_f + 2\mu)\nabla^2\mathbf{u} - \mu\nabla\times\nabla\times\mathbf{u} - \rho_m = a\phi\rho_f\ddot{u} - a\phi\rho_f\ddot{\mathbf{U}} + b(\dot{\mathbf{u}} - \dot{\mathbf{U}}).$$

The right-hand-side term of the two equations are equal. Consequently, the left hand expression of the second equation is zero, which is the standard wave equation for single phase solids.

Without Dissipation – $b = 0$ which implies transmissibility $\gamma = \inf$ or porosity $\phi = 0$ – Biot's wave equation for porous rocks predicts two P-waves. For P-waves we can express the displacements $\mathbf{u}$ and $\mathbf{U}$ as gradients of a potential Φ:

$$\begin{bmatrix} \mathbf{u} \\ \mathbf{U} \end{bmatrix} = \begin{bmatrix} \nabla\Phi \\ \nabla\Phi \end{bmatrix} = \nabla\Phi. \tag{31}$$

Consequently, $\nabla\times\mathbf{u} = \nabla\times\mathbf{U} = \mathbf{0}$ and the wave equation expressions 30 reduce to

$$\tilde{R}\nabla^2\Phi - \tilde{M}\ddot{\Phi} = 0$$

where

$$\tilde{R} = \begin{bmatrix} \lambda + 2\mu & Y \\ Y & R \end{bmatrix}, \tilde{M} = \begin{bmatrix} \rho_{11} & \rho_{12} \\ \rho_{12} & \rho_{22} \end{bmatrix}.$$

The matrix $\tilde{R}^{-1}\tilde{M}$ is positive definite and consequently has two real eigenvalues v_{p1} and v_{p2}. In the matrix's eigenvector reference system, the wave equation reduces to

$$\nabla^2 \Phi^\star - \begin{bmatrix} \frac{1}{v_{p1}} & 0 \\ 0 & \frac{1}{v_{p2}} \end{bmatrix} \ddot{\Phi}^\star = 0$$

where $\Phi^\star$ is the potential function in the eigenvector reference system. The equation implies two decoupled P-waves. The second P-wave velocity v_{p2} is usually significantly smaller than the first. The faster v_{p1} merges with the classic P-wave in the absence of pore fluids.

Analogues introducing shear waves

$$\begin{bmatrix} \mathbf{u} \\ \mathbf{U} \end{bmatrix} = \begin{bmatrix} \nabla \times \Theta \\ \nabla \times \Theta \end{bmatrix} = \nabla \times \Theta. \tag{32}$$

we find a single shear wave with velocity

$$v_s = \left(\frac{\mu}{\rho_{11} - \frac{\rho_{12}^2}{\rho_{22}}} \right)^{\frac{1}{2}}.$$

The fluid influences the shear velocity indirectly due to its effect on the overall inertia of the porous rock.

With dissipation the P-Wave ansatz 31 reduces the general wave equation 30 to

$$\tilde{R}\nabla^2\Phi^2 = \tilde{A}\dot{\Phi} + \tilde{M}\ddot{\Phi} \tag{33}$$

where $\tilde{A}$ is the damping matrix

$$\tilde{A} = \begin{bmatrix} b & -b \\ -b & b \end{bmatrix}.$$

The ansatz for harmonic P-waves is

$$\Phi_1 = \Phi_{10} \exp i(\mathbf{kx} - \omega t) \tag{34}$$
$$\Phi_2 = \Phi_{20} \exp i(\mathbf{kx} - \omega t) \tag{35}$$
$$\tag{36}$$

where Φ_{10} and Φ_{20} are constant and ω and $\mathbf{k}$ are the angular frequency and the wave number. The introduction of this ansatz into the wave equation **??** yields a system of two equation. To ensure that a solution exists the determinant of the homogeneous system has to be zero. This condition leads to dispersion relationships with two solutions: k_{P1} and k_{P2} which relate to the two types of P-waves found in the case without dissipation. Both wave numbers are complex. The real part describes the harmonic propagation:

$$Re(k_{Pi})\, v_{Pi} = \omega.$$

where v_{Pi} relates to the velocities found in the non-dissipating discussion. The complex part governs the amplitude dissipation of the wave. The propagation velocity is dispersive since frequency dependent. As the frequency approaches zero, the source of dissipation – the relative motion between the fluid and the matrix – vanishes. At frequencies where $\tilde{M}\ddot{\Phi}$ can be ignored, the equation, once more, reduces to Darcy's law of steady flow.

In summary, Biot's model yields a consistent and analytic solution to the propagation of waves in porous media. Its results are backed by laboratory confirmations at a wide variety of rock samples. Unfortunately, its velocity expressions are rather complicated.

Terzaghi's model

Terzaghi simplifies Biot's model by decoupling the stress tensor into hydrostatic stress and stresses of the solid skeleton. Terzaghi's approximation, which are popular in the field of geomechanics, imply

$$\begin{aligned} \beta &= \phi && (37) \\ K_f &= K_s(1-\phi) + K_f\phi && (38) \\ M &= K_f/\phi && (39) \\ p &= -K_f \nabla \mathbf{U} && (40) \\ & && (41) \end{aligned}$$

If we further assume that the tortuosity $a = 1$ is one and that we can ignore dissipation due to viscosity, we find again two non-dissipative P-waves with velocities

$$v_{P1} = \left(\frac{\lambda_0 + 2\mu}{\rho_2(1-\phi)} \right)^{1/2} \quad (42)$$

$$v_{P2} = \left(\frac{K_f}{\rho_f} \right)^{1/2} . \quad (43)$$

The first P-wave only involves the rock matrix, the second only involves the fluid.

If we continue to ignore loss due to viscosity but allow for tortuosity $a \neq 1$ and a fluid bulk modulo much smaller than the solid bulk modulo ($K_f \ll K_m$) than the wave velocities are

$$v_{P1} = \left(\frac{\lambda_0 + 2\mu}{\rho_s(1-\phi) + \phi\rho_f(1-a^{-1})} \right)^{1/2} \quad (44)$$

$$v_{P2} = \left(\frac{K_f}{a\rho_f} \right)^{1/2} \quad (45)$$

$$v_s = \left(\frac{\mu}{\rho_s(1-\phi) + \phi\rho_f(1-a^{-1})} \right)^{1/2} \quad (46)$$

But Tzeraghi's assumption of decoupled stresses is considered unrealistic for usually highly consolidated hydrocarbon reservoir rocks.

Wyllie's model

For many years, traditional seismic processing approximated the propagation of seismic waves by the acoustic wave equation 18. Wyllie (1956) suggested a simple empirical time-average equation to relate the wave's phase velocity v to porosity ϕ, fluid velocity v_f, and rock matrix velocity v_m:

$$\frac{1}{v} = \frac{\phi}{v_f} + \frac{1-\phi}{v_m} \tag{47}$$

This relationship was used extensively in the interpretation of sonic well log measurements. Raymer (1980) suggests an improved expression for sandstones.

GENERAL INVERSION THEORY

simple example? gravimetry falling object.

What does a scientist do? A scientist observes, explains, predicts, and publishes. Scientists ultimately observe nature. The fundamental insight that nature's laws are universal, allows a scientist to simplify complex nature into simpler experiments. To qualify as scientific, the experiments and observations have to be reproducible by other interested scientists.

The scientist then employs a scientific theory to *explain* the observations. Such theories tend to be mathematical laws that combine a set of parameters that describe nature's state to the observed quantities.

From all the models that might explain an observations, a scientist chooses the most parsimonious model. In many cases, a scientist has to choose among several computational models. Quantum versus Newtonian mechanics, pixel versus graphical object parameterization, or L_1 versus L_2 norm are classic cases of competing mathematical models. Additionally, practical considerations, such as computational cost and implementation time, may influence a scientist's choice.

A scientific theory is usually used in two ways: forward and backwards. Most of the time actually both ways, simultaneously. To test a scientific theory, a scientist predicts an experiment's observation from the experimentally controlled state of the system of interest. If the best fitting predicted data of a mathematical model does not fit the observed data, then the scientist needs to find an improved theory. Such a replacement usually involves a better approximation of the underlying physics (an acoustic wave equation is replaced by an elastic one, or quantum effects are taken into account). Interestingly the improved models usually extend the traditional ones. The traditional models are not wrong but remain useful approximations of the improved theory in the traditional cases.

Observations and a scientific model of nature can also be used to deduce the state of nature under observation. Once a scientist decides on a computational model numerical analysis devises methods to approximate the optimal estimate of the model parameters from the given observations. Interestingly, the forward simulation is usually simpler than its inversion: a case of scrambling of information or, for the more metaphysically inclined, an application of the second law of thermo dynamics.

Furthermore, a computational model suggests an experiment that resolves parameters of the model optimally.

Seismic. In general, I believe inversion continues to be a fruitful source of innovation in geophysics. Inversion theory distinguishes model formulations. Inversion theory guides the design of optimal acquisition geometry. Finally, inversion leads to an optimal approximation of model parameters. I expect succesfull traditional processing approaches to reappear as individual approximative steps of corresponding inversion formulations.

Integration of experiments

The integrated formulation of two related experiments promises the consistency of the simulation and inversion results. The combination of parameters estimates, such as maximum likelihood points or mean value of an distribution, derived from the inversion of two separate inversions, leads to biases in the solution. On the other hand, the complete probability distribution of the two solutions could be combined correctly. However, assigning and handling proper probability distributions is difficult. The integrated and simultaneous inversion of both experiments leads to unbiased estimates. Additionally, the inversion allows a scientist to integrate a wide variety of experiments, including seismic time-lapse surveys that differ in geometry and instrumentation.

Limitations of integration. The integration of various experiments into a single inversion is conceptually simple and optimal, but poses several severe practical problems. For example, where should integration stop? An ambitious manager may want to include economic considerations and optimize for profit rather than for subsurface parameters. While I believe that such a formulation is actually desirable, I doubt the problem can be implemented successfully today.

Only the data of closely related experiments should be combined to an integrated inversion, for example, experiments that resolve the same model parameters, or the model parameters are related by well known direct physical relationship. Problems that are not at all or loosely connected should probably be simulated and inverted in separate computations.

Additionally, computational size and the availability and cost of compute time will limit our capability to integrate. The inversions of a series of small problems are less expensive than the inversion of the integrated problem.

Finally, the experts for each experiment need to collaborate in the integration of the experiment. I believe that flexible a software framework (Schwab and Schroeder, 1997) can facilitate easy integration of the various experiments without unduly burdening the individual expert scientist.

FUTURE WORK

[3]

Much of my current implementation of reservoir flow and wave propagation simulation begs to be improved: Multiphase flow simulations, Gassmann's expressions sensibly relating reservoir properties to wave velocity expressions, elastic wave simulator.

However, priority should be the implementation of the corresponding inversion. An existing inversion implementation that resolves reservoir properties from given observations should serve as a guide in choosing appropiate and beneficial subsequent improvements. Ultimately, tests on field data will probably require savvy implementations of the reservoir flow and wave simulator. Additionally, I would want to include well log measurements into the inversion for reservoir properties.

I would like to improve my Java finite difference operators to a versatile object-oriented hierarchy that has the same flexibility as Karrenbach's Genmod modelling code.

Game. Ideally, this article would include an interactive Java game. A player would operate an unknown oil field. Starting with a given budget, the player invests his money into seismic surveys and wells. The player chooses a well location, pays for the drilling of a well, and decides on the pressure in the well during production. Each barrel produced by a player's well adds to his budget. Additionally, the player can conduct seismic seismic experiments and well tests for a fee. The surveys yield estimates of reservoir properties such as saturation, pressure distribution, etc. If the player successfully exploits the reservoir without going bankrupt, a more complex prospect is offered. A score list compares various players success as operators.

CONCLUSIONS

I advocate to integrate all observations of a reservoirs into a single inversion for parameters. Seismic time lapse surveys are sensitive to saturation changes and, consequently, overlap with other subsurface measurements, such as the petroleum engineer's well tests. A joint inversion guarantees a consistent estimate and a framework of interpretation. Furthermore, the interference of independent information introduces new constraints and may make an integrated inversion feasible.

The integration may change traditional acquisition design, subsurface parameterization, and processing of the available observations. The various experiments ought to be reevaluated with respect to their contribution to the overall resolution of unknown reservoir properties. Overall, the inversion framework should help scientists to improve and harmonize the various experiments. In practice, the shear size of an integrated inversion may require separate inversions of the various data types. However, integrated studies should clarify the conceptual formulation. Any practical approximations and shortcuts should be chosen with a clear understanding of their consequences.

---
[3]In this section, I list what ought to be done next to further this research, not necessarily what I will do.

The current approach of interpreting difference sections of time-lapse experiments is an incomplete formulation of the underlying inversion problem. One might describe it as a first step of the more comprehensive inversion. I believe, that a clever approach to the integrated inversion may, however, very well include the formulation of such difference sections. I wonder if Symes' Difference Semblance Optimization (1991) could be extended to the time-lapse formulation.

This document discussed simulation models and partial differential equations for wave and fluid propagation in porous rocks. Among several alternative models, I emphasized Gassmann's model of elasticity and Darcy's fluid flow model for black oil. The models share similar parameterization and degree of parsimony. However, I implemented starkly simplified finite difference algorithms for both experiments. A future inversion of the simplified simulators should guide any necessary improvement of my implementations.

REFERENCES

Aki, K., and Richards, P. G., 1980, Quantitative seismology: Theory and methods: W. H. Freeman and Co., New York.

Aziz, K., and Settari, A., 1979, Petroleum reservoir simulation: Applied Science Publishers.

Berryman, J. G., 1980, Confirmation of biot's theory: Applied Physical Letters, **37**, 382–384.

Biondi, B., Lumley, D., Mavko, G., Mukerji, T., Rickett, J., Deutsch, C., Gundeso, R., and Thiele, M., 1996, Reservoir monitoring: A multi-disciplinary feasibility study: Stanford Rock Physics Project–

Biot, M. A., 1962, Mechanics of deformation and acoustinc propagation in porous media: J. Appl. Mech., **23**, 1482–1498.

Bourbie, T., Coussy, O., and Zinszner, B., 1987, Acoustics of porous media: Gulf Publishing Company.

Clayton, R. W., and Engquist, B., 1980, Absorbing side boundary conditions for wave equation migration: Geophysics, **45**, no. 5, 895–904.

Landa, J. L., 1997, Reservoir parameter estimation constrained to pressure transients, performance history, and distributed saturation data: Stanford Petroleum Engineering Department–

Lumley, D. E., 1995, 4-d seismic steamflood monitoring: SEP–**89**, 25–72.

Mindlin, R. D., 1949, Compliance of elastic bodies in contact: Trans. ASME, A–259.

Raghavan, R., 1993, Well test analysis: Prentic Hall.

Raymer, L. L., Hunt, E. R., and Gardner, J. S., 1980, An improved sonic transit-time-porosity transform: Soc. Prof. Well Log Analysts, 21st Annual Logging Symposium Transactions.

Schwab, M., and Schroeder, J. M., 1997, Jest, an optimization library: `http://sepwww.stanford.edu/sep/matt/jest`.

Symes, W. W., and Carazzone, J. J., 1991, Velocity inversion by differential semblance optimization: Geophysics, **56**, no. 5, 654–663.

Wyllie, M. R. J., Gregory, A. R., and Gardner, L. W., 1956, Elastic wave velocities in heterogeneous and porous media: Geophysics, **21**, no. 1, 41–70.

ODDYSEE OF A PROJECT

Settling on a project I had intended to implement Bill Symes (cite) Differential Semblance Optimization for plane wave estimation. I abandoned the project, since Symes approach is an inversion problem and has no intrinsic relation to wave propagation. As Symes emphasizes in his paper, the inversion approach is applicable for any *multi-experiment* data fitting. The physical process underlying the experiment is irrelevant. Plane wave estimation is just one example. Furthermore, the implementation proved more difficult than I had assumed.

In search of a new topic, I considered the approximation of the Zoeppritz equation for reflected and transmitted waves. The topic fitted the course, a former professor of mine, Dr. Bortfeld, wrote a classic paper (**?**) on the topic, and industry interest in AVO may benefit me later. However, I was not enthused by an entirely theoretical paper (even if it were to include a few Mathematica figures). Ultimately, I decided to approach a more applied angle of the AVO and Zoeppritz problem.

Professor Horne's[4] presentation on estimating reservoir parameters from seismic and well data lead to my attempt to integrate the experiments of the petroleum engineer and the geophysicist in a single formulation. I especially intended to incorporate the seismic raw data rather than the interpreted seismic events.

Appendix: Zoeppritz

In the current project, I simply model the wave propagation in a porous rock. In the future, I want to invert recorded seismograms to estimate the subsurface properties. In general, I could attempt to find the inverse operator to the wave propagation simulator. Traditionally, it was useful to approximate seismic inversion by two separate estimations of the subsurface velocity and the reflectivity. The pore fluids effect on velocities we explicitly derived in the previous sections. Their effect on amplitudes is not explicit in the equations above.

Studies of amplitude-versus-offset formulate the amplitude behavior of seismic reflections explicitly. The derivation is based on the Zoeppritz equations for reflected and transmitted amplitudes at concrete interfaces. Zoeppritz requires the continuity of displacement and stress (acceleration) at the interface and derives a matrix equation for the amplitude of waves at any impedance angle. The matrix coefficients depend on P-, S-wave velocity, and density, which in turn are dependent on lithology, porosity, pore fluid content, and temperature. Bortfeld (**?**), and Aki (1980) have published scalar approximations to the matrix equation usually based on the assumption of small incident angles.

In sophisticated AVO studies, the amplitude changes with offset (or more correctly with angle) are translated into *hydrocarbon indicators*. Considering the success of this approach, it seems attractive to use a similar formulation in time-lapse processing. To integrate the time-lapse experiments with petroleum engineering the AVO inversion needs to resolve physical parameters, such as saturation, rather than a generic hydrocarbon indicator.

[4] Stanford Petroleum Engineering Department

Since Zoeppritz equations are based on discrete interfaces, the AVO approach comes natural for models that are parameterized as objects. To apply an AVO analysis to a subsurface model parameterized by pixels requires the explicit or implicit estimation of the local reflector slope and the specular reflection.

Failure viscous elastic formulation

I designed a small object-oriented finite difference library. The idea was to have a set of basic operators that I can combine to more complex ones. In the case of the wave equation, I intended to build the operator from operators that implement the equation of state, motion, and viscosity.

I gave up on this approach, when I could not find stable parameters for the explicit formulation of the scalar acoustic wave propagation in viscous material. Building the wave equation from basic operators lead to a rather complex condition for stability, as I will show below. I did not expect the stability analysis for the compounded wave operator to be more complex than the analysis for the standard implementation. Anyway, here is what I found until I abandoned the project:

The derivation of the acoustic wave equation is based on the combination of three equations that have physical meaning by themselves. The **continuity equation** describes the excess mass flow due to the divergence of $\rho\mathbf{v}$, the local density and material velocity:

$$-\dot{\epsilon} = \nabla(\rho\mathbf{v}). \tag{48}$$

(Obviously, an excess in mass flow changes the density: the density is defined as time average, so that $\rho_{total} = \rho + \rho_e = \rho(1+\epsilon)$.) The **equation of state** relates the change in excess pressure σ to a change in excess density ϵ. For elastic behavior, the equation is simply Hook's law $\sigma = c\epsilon$. The elastic description of Hook's law is a good approximation for many materials and situations. However, the approximation has obvious shortcomings, e.g. the response to pressure is instantaneous, reversible, and without friction loss. An improvement, albeit still an idealized approximation, is the viscous equation of state

$$\sigma = c\epsilon + \eta\dot{\epsilon} \tag{49}$$

which accounts for a time delay in change of excess density. Finally the **equation of motion** encapsulates Newton's second law $\mathbf{F} = m\dot{\mathbf{v}}$. In our formulation it relates a change in material velocity to the change in excess pressure,

$$\rho\dot{\mathbf{v}} = -\nabla\sigma. \tag{50}$$

The three equations do constitute the wave equation. The substitution of $\dot{\epsilon}$ in the equation of state by the corresponding expression in the equation of continuity 48, yields

$$\sigma = c\epsilon - \eta\nabla(\rho\mathbf{v}).$$

The partial time derivative of the expression is

$$\dot{\sigma} = c\dot{\epsilon} - \eta\nabla(\rho\dot{\mathbf{v}}).$$

where I interchanged the order of differentiation assuming well-behaved solutions. Substitution of $\dot{\mathbf{v}}$ by an expression derived from the equation of motion 50 yields

$$\dot{\sigma} = -c\nabla(\rho\mathbf{v}) + \eta\nabla^2\sigma.$$

Finally, the partial time derivative of this expression

$$\ddot{\sigma} = -c\nabla(\rho\dot{\mathbf{v}}) + \eta\nabla^2\dot{\sigma}$$

and the divergence of the equation of motion 50

$$\nabla(\rho\dot{\mathbf{v}}) = -\nabla^2\sigma$$

allow us to eliminate the velocity term and yield the viscous wave equation for the material's pressure

$$\ddot{\sigma} = c\nabla^2\sigma + \eta\nabla^2\dot{\sigma}.$$

Instead of implementing the wave equation directly, I decided to implement a system of three partial differential equations of which each equation has its own meaning and application. The elastic part of equation of state 49 and the continuity equation 48 combine to

$$\frac{\dot{\sigma}}{c} = -\nabla(\rho\mathbf{v}). \tag{51}$$

The viscous part of the equation of state is formulated as an independent heat equation

$$\dot{\sigma} = \eta\nabla^2\sigma. \tag{52}$$

The equation of motion stays unchanged[5].

The discrete version of the combined state and continuity equation 51 is

$$\sigma_{t+1}^{x,y} = \sigma_t^{x,y} - \frac{c\rho\Delta t}{\Delta x}[(u_t^{x,y} - u_t^{x-1,y}) + (v_t^{x,y} - v_t^{x,y-1})]$$

where $\mathbf{v} = (u, v)$ are the components of the velocity vector in two dimensions, the superscript indicates the spatial sample, the subscript indicates the temporal sample, and Δt and Δx are the respective discrete increments between samples. In two dimensions, the equation of motion 50 has two components

$$\begin{aligned} u_{t+1}^{x,y} &= u_t^{x,y} - \frac{\Delta t}{\rho\Delta x}[\sigma_t^{x+1,y} - \sigma_t^{x,y}] \\ v_{t+1}^{x,y} &= v_t^{x,y} - \frac{\Delta t}{\rho\Delta x}[\sigma_t^{x,y+1} - \sigma_t^{x,y}]. \end{aligned}$$

Finally, the discretization of the heat equation 52 yields

$$\sigma_{t+1}^{x,y} = \sigma_t^{x,y} - \frac{\eta\Delta t}{\Delta x^2}[(\sigma_t^{x-1,y} - 2\sigma_t^{x,y} + \sigma_t^{x+1,y}) + (\sigma_t^{x,y-1} - 2\sigma_t^{x,y} + \sigma_t^{x,y+1})].$$

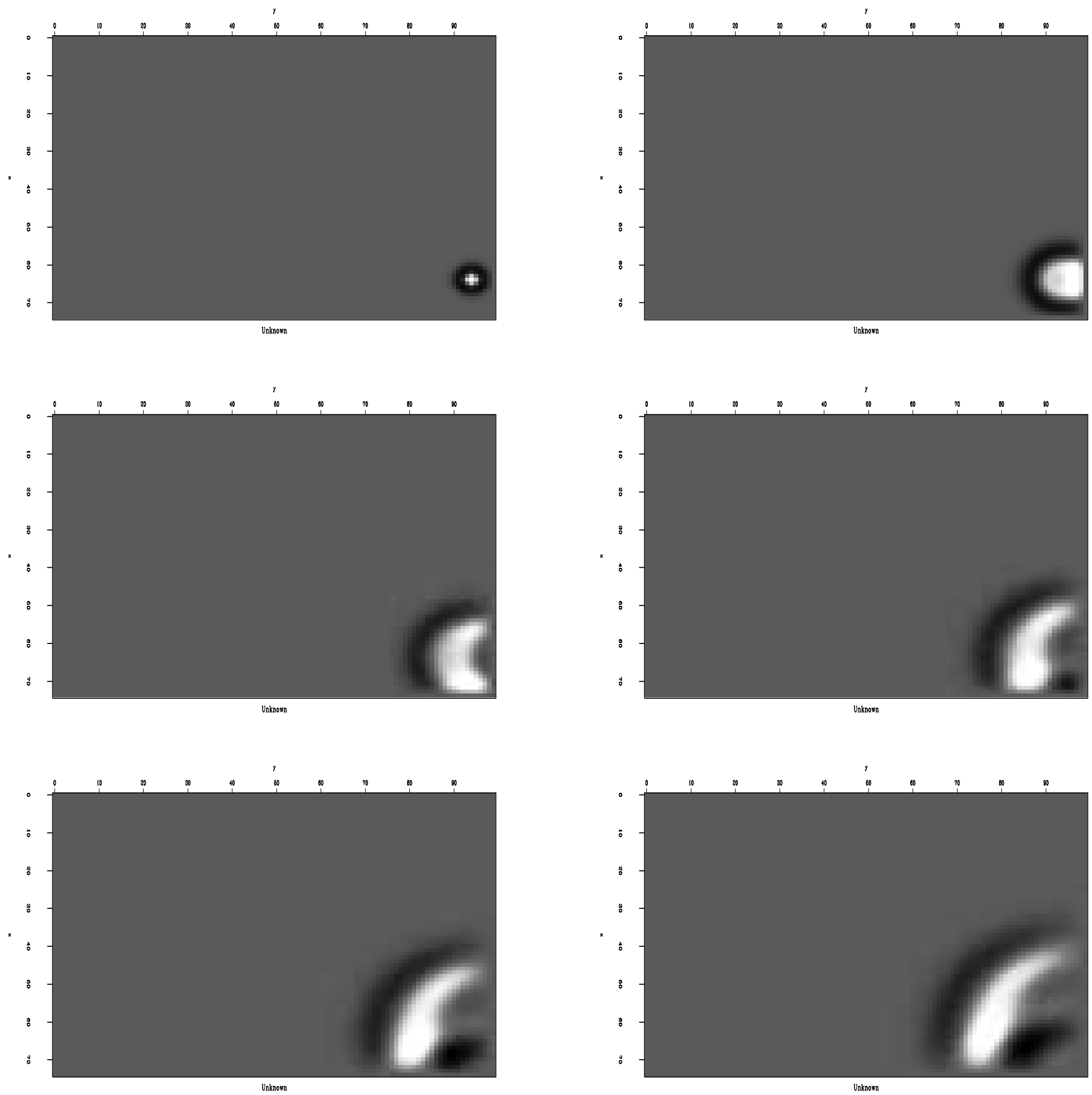

Figure 9: Snapshots of the viscous elastic wave equation simulator. The simulator is instable. $\boxed{\text{frog}}$ [ER]

I programmed the three equations, and Figure 9 shows snapshots for a point source and progressing time. The later frames show the computation to be instable, a standard problem with explicit finite difference schemes. I first tried to guess parameters η, c, and ρ for which the computation would be stable. I mostly increased the viscosity to counteract the exponential amplitude growth by exponential amplitude reduction. When I failed to find appropriate values, I decided to estimate the stability limits of the parameters by careful analysis of the Courant-Levy criteria.

The eigenmodes of the discrete equation system are

$$\begin{bmatrix} \sigma_t^{x,y} \\ u_t^{x,y} \\ v_t^{x,y} \end{bmatrix} = \xi^t e^{ik_x j\Delta x} e^{ik_y l\Delta y} \begin{bmatrix} \sigma_0 \\ u_0 \\ v_0 \end{bmatrix}.$$

Substitution of the right hand side in the system of difference equations (now written as a matrix operator) yields

$$\begin{bmatrix} 0 \\ 0 \\ 0 \end{bmatrix} = \left[\begin{matrix} 2 + \hat{\eta}(e^{-ik_x\Delta x} - 2 + e^{ik_x\Delta x} + e^{-ik_y\Delta y} - 2 + e^{ik_y\Delta y}) - \xi & -\hat{K}(1 - e^{-ik_x\Delta x}) & -\hat{K}(1 - e^{-ik_y\Delta \\ -\hat{p}(e^{ik_x\delta x} - 1) & 1 - \xi & 0 \\ -\hat{p}(e^{ik_y\delta y} - 1) & 0 & 1 - \xi \end{matrix} \right.$$

where

$$\hat{\eta} = \frac{\eta\Delta t}{\Delta x^2}, \hat{K} = \frac{c\rho\Delta t}{2\Delta x}, \hat{p} = \frac{\Delta t}{\rho\Delta x} = \frac{\Delta t}{\rho\Delta y}.$$

To find the stability limit, I need to find parameters $\eta, c, \rho, \Delta x$, and Δt so that all the eigenvalues of the propagation matrix are smaller than 1. This is equivalent with ensuring that the values of ξ for which the determinant of the matrix is zero are all smaller than 1. The limit has to hold for all wave numbers k_x and k_y. The determinant is a third order polynomial in ξ and the estimation of the upper limit requires very careful accounting of the sign of all the exponential expressions. When I first investigated the problem, I was stumped. But now I realize that I can find the boundaries by computing the zeroes of the corresponding derivatives and by checking the particular boundary values. The computation is tiresome but feasible. I, however, had already moved on and implemented the simpler acoustic wave equation.

[5]Note, that the equation of state and continuity 51 and the heat equation 52 have to be added. I wonder if I do that correctly.